J Neurol (2013) 260:540–548
DOI 10.1007/s00415-012-6674-4

ORIGINAL COMMUNICATION

# Hirayama disease is a pure spinal motor neuron disorder—a combined DTI and transcranial magnetic stimulation study

**Kai Boelmans · Jörn Kaufmann · Sophie Schmelzer · Stefan Vielhaber · Malte Kornhuber · Alexander Münchau · Stephan Zierz · Charly Gaul**

Received: 6 April 2012 / Revised: 27 August 2012 / Accepted: 7 September 2012 / Published online: 25 September 2012


**Abstract** Hirayama disease (HirD) is a juvenile spinal muscular atrophy predominantly affecting young men with an initially progressive course followed by a stable plateau within several years. It is a matter of debate whether HirD is a widespread motor neuron or more focal cervical cord disease. Whether the supraspinal pathways of the corticospinal tract (CST) are also affected has not been studied systematically. We analyzed CST integrity in seven HirD patients and 11 controls of similar age and gender using diffusion tensor imaging at a 1.5-T scanner and central motor conduction time (CMCT) using transcranial magnetic stimulation. The apparent diffusion coefficient, fractional anisotropy, and axial and radial diffusivity coefficients were determined bilaterally at four representative CST levels and along the whole CST using a probabilistic fiber tracking approach. There were no differences between the initially affected and the contralateral side in HirD patients and no difference between HirD patients and controls for both the ROI-based and the whole CST analyses. Radial diffusivity of the CST was positively correlated with years of disease progression in HirD patients. CMCT was normal in HirD patients. Combined anatomical and functional measurements established normal integrity of the supraspinal CST in HirD patients lending support to the notion that HirD is a pure spinal motor neuron disorder.

**Keywords** Hirayama disease · Corticospinal tract · Diffusion tensor imaging · Fiber tractography · Motor evoked potentials

K. Boelmans (✉)
Department of Psychiatry, Memory Clinic, University Hospital Hamburg-Eppendorf, Martinistrasse 52, 20246 Hamburg, Germany
e-mail: k.boelmans@uke.uni-hamburg.de

K. Boelmans · J. Kaufmann · S. Vielhaber
Department of Neurology, Otto-von-Guericke-University, Magdeburg, Germany

S. Schmelzer · M. Kornhuber · S. Zierz · C. Gaul
Department of Neurology, Martin-Luther-University Halle-Wittenberg, Halle (Saale), Germany

A. Münchau
Department of Neurology, University Hospital Hamburg-Eppendorf, Hamburg, Germany

## Introduction

Hirayama disease (HirD), or benign juvenile muscular atrophy of distal upper extremity, is characterized by muscular weakness and atrophy in the hand and forearm, predominantly affecting young men [1]. The pattern of atrophy involves the volar and dorsal surfaces of the forearm, sparing the brachioradialis muscle, also referred to as "oblique amyotrophy" [2]. The course of HirD is initially progressive with an insidious onset between the second and early third decade of life, followed by spontaneous stabilization within several years. HirD patients as a rule do not have pyramidal signs indicative of corticospinal tract (CST) involvement [2, 3]. However, in selected cases, lower limb hyperreflexia has been described [4–6], which might point towards subtle CST dysfunction. Position-dependent microcirculatory disturbance in the territory of the anterior spinal artery has been postulated as one of the mechanisms leading to degeneration of anterior horn cells in HirD (flexion induced myelopathy) [2, 7]. Various magnetic resonance imaging (MRI) investigations have lent support to this hypothesis showing a dynamic

compression of the lower cervical cord due to forward displacement of the dural sac and spinal cord during neck flexion [8–11]. However, due to conflicting results, HirD has alternatively been viewed as an intrinsic motor neuron disease because a number of HirD cases without evidence of flexion induced myelopathy have been reported [12–16] and because of reports of familial cases [14, 17]. If so, then CST involvement would indicate a more widespread motor neuron disease.

To this end, we investigated a potential involvement of the supraspinal CST in clinically stabilized HirD patients using MR-based diffusion tensor imaging (DTI) and transcranial magnetic stimulation (TMS). The aim of this study was to examine whether HirD is a more widespread or pure spinal motor neuron disease.

## Patients and methods

### Participants

Seven HirD patients (mean age 33 ± 13.9 years, range 19–55, five males) from the Departments of Neurology at the University Hospitals of Halle and Magdeburg participated in the study. HirD was made according to the predefined criteria: (1) atrophy and weakness in one distal upper limb or asymmetrically in both, (2) insidious onset in the second or third decade of life, (3) initial fast progression followed by a stable condition, (4) no involvement of cranial nerves, sensory, cerebellar or extrapyramidal systems and cortical functions, (5) no history of poliomyelitis, (6) no family history of other neuromuscular diseases [7, 11, 18].

Electrophysiological and MRI investigations were carried out in all patients during stabilization of the disease. Eleven healthy subjects (mean age 31 ± 12.0 years, range 18–54, seven males) without any neurological or psychiatric signs were recruited as a control group. Five patients and 11 controls were right handed, one patient was left handed (no. 4) and one had switched from left to right hand in childhood for reasons unrelated to HirD (no. 3). The study was approved by the local ethics committee and is in accordance with the ethical standards of the Declaration of Helsinki. All participants gave written informed consent before study participation.

### Motor evoked potentials

Motor evoked potentials (MEP) recordings were obtained by TMS over the motor cortex using a conventional round coil connected to a stimulator (MagStim 2000, inner diameter 13 cm, Viasys, Höchberg, Germany) producing a maximum magnetic field of 2.0 T. The circular copper coil was placed on the skull vertex and over the L5 spinous process. Surface electromyography (EMG) responses were recorded from the tibialis anterior muscle bilaterally. TMS intensity was set at 20–30 % above the resting motor threshold, which was defined as the minimum stimulus intensity at which five of ten consecutive stimuli evoked MEP amplitudes of at least 50 μV in the relaxed tibialis anterior muscle. Central motor conduction times (CMCT) were calculated by subtracting the latency in response to spinal root stimulation from the latency in response to cortical stimulation.

### Nerve conduction studies and electromyography

Electrophysiological recordings were carried out under standard conditions on a multiliner machine (Viasys, Höchberg, Germany). M- and F-waves were recorded from motor fibres of the ulnar nerve using supramaximal stimulation. For F-wave generation, the nerve was repeatedly (ten times) and supramaximally stimulated. Distance between stimulation cathode and C7 was measured and motor nerve conduction velocity (NCV), amplitudes, distal latency as well as amplitudes, persistence, and temporal dispersion of F-waves analyzed. Sensory action potentials of the ulnar nerve were derived from sensory nerve conduction studies (NCS) using ten antidromic stimuli with subsequent averaging. The distance between the cathode and recording electrode was measured and sensory NCV, amplitudes, and latencies analyzed. For somatosensory evoked potentials, recording electrodes were placed on the scalp (C3 and C4) and over the cervical spine (C7). The ulnar nerve was stimulated bilaterally at the wrist with 1,000 stimuli to extract the SSEP from the background activity by averaging. Impulses showed intensities between 10 and 20 mA and were individually adapted to the motor threshold of digiti minimi muscles. Latencies and amplitudes of the central peaks (N20, P25, and N1) were measured. To measure the sympathetic skin responses, surface plate electrodes were used and the skin was cleaned for low skin resistance. The recording electrode was placed in the palm and the reference electrode positioned on the dorsal side of the hand. Three stimuli were triggered at 30 mA at the left upper arm and responses recorded on the ipsi- and contralateral side, respectively. Electromyography was recorded in all the patients using concentric needles and standard techniques.

### Image acquisition and processing

The MRI was performed using a GE Signa LX 1.5-T system (General Electric, Milwaukee, WI, USA) with actively shielded magnetic field gradients (maximum amplitude 40 mT $m^{-1}$). A standard quadrature birdcage

head coil was used for both the radio-frequency transmission and signal reception. The MR protocol included a T1-weighted sagittal 3D scan (contrast-optimized spoiled gradient-echo sequence; 124 slices, slice thickness 1.5 mm; TE 8 ms; TR 24 ms; flip angle 30°) and a single-shot diffusion-weighted spin-echo-refocused echoplanar imaging sequence (data acquisition matrix 128 × 128; field of view 280 × 280 mm; TE 70 ms; TR 10.000 ms; 39 slices; slice thickness 3 mm; b-value 1,000 s/mm$^2$).

The data for diffusion tensor calculations were collected with 12 noncollinear gradient orientations, each additionally measured with the opposite diffusion gradient polarity [19]. The orientations were chosen according to the DTI acquisition scheme proposed by Papadakis and colleagues [20]. The total of 24 diffusion-weighted measurements, each an average of four measurements, were divided into four blocks, each preceded by a non-diffusion-weighted acquisition. Diffusion tensor imaging volumes were eddy-current and head motion corrected based on the non-diffusion-weighted images using the AIR software package [19, 21]. Diffusion tensors were calculated for each voxel and further decomposed into eigenvalues and eigenvectors. On the basis of the eigenvalues, the apparent diffusion coefficient (ADC) and fractional anisotropy (FA) as well as the axial diffusivity (AD) and radial diffusivity (RD) coefficients were determined. Diffusion tensor imaging-based color maps were calculated according to the scheme proposed by Pajevic and Pierpaoli [22]. The fiber tract reconstruction was carried out using a probabilistic approach. A Monte Carlo simulation algorithm that repeatedly searches for probable paths through the derived diffusion tensor matrix was implemented in MATLAB (MathWorks, Natick, MA, USA) [23].

Diffusion tensor imaging is particularly sensitive to assess in vivo the tissue characteristics along white matter tracts [24]. The principle is based on a non-invasive measurement of the random movement of water molecules. As the water tends to diffuse preferentially along ordered structures such as axonal tracts, DTI can provide detailed information about white matter integrity [25]. Two scalar measures, which can be extracted in a voxel-wise manner, are the ADC, which represents the magnitude of local diffusion averaged over all spatial directions, and the FA, which quantifies the degree of anisotropy. Additionally, the axial (parallel to the long axis of fiber) and radial (perpendicular) diffusivity coefficients may provide complementary information regarding tissue microstructure in white matter tracts [26].

Regions of interest (ROIs) based DTI parameters were manually determined in all seven HirD patients and 11 control subjects at four different levels along the CST [capsula interna (43.1 mm$^2$), cerebral peduncle (28.7 mm$^2$), pons (10.7 mm$^2$), and pyramids (7.2 mm$^2$)] in each hemisphere (Fig. 1). Regions-of-interest sizes and positions were kept identical between the subjects. For fiber tractography, seed points with a size of 3.3 × 3.3 mm$^2$ were placed within each hemisphere at the level of the medulla oblongata. Tractography analysis of the CST was performed independently with 50,000 starts in the left and right hemisphere. Clustering was conducted on the basis of distance criteria. Tract-specific diffusion parameters were determined for left and right CST by marking the voxels traversed by any counted path. For interhemispheric and group comparisons, each subject's diffusion parameters were averaged over all marked voxels in the neuronal tract being evaluated.

### Statistical analysis

Data were analyzed using the SPSS software package for Windows (version 15.0; SPSS Inc., Chicago, IL, USA). Between-group differences in gender distribution were analyzed with $\chi^2$ tests; differences in age were analyzed using the Mann–Whitney $U$ test. Correlations of CST diffusion parameters with years of disease progression, age, and CMCT were investigated by using the Pearson's correlation coefficient. Normal distribution was confirmed by Shapiro–Wilk test. Adapted from the ROI-based and tract-specific diffusion parameters, the mean of diffusion values was determined for further statistical analysis. Analyses of variance (ANOVAs) were performed to test for differences of both ROI-based and tract-specific diffusion parameters.

## Results

### Demographical and clinical data

There were no significant differences in gender distribution or age between HirD patients and control subjects. Demographical and clinical data of HirD patients are summarized in Table 1.

### Cervical MRI findings

Each patient except one (no. 3, computed tomography) received a neutral-position cervical MRI that showed a normal width of the cervical spinal cord. In addition, no lower cervical cord atrophy, asymmetric cord flattening, or abnormal cervical curvature could be detected. Three patients (no. 1, 3, and 5) showed degenerative changes of the cervical spine as spondylosis deformans and uncarthrosis.

### Electrophysiological findings

Central motor conduction time was normal in six patients; it could not be calculated in one patient (no. 2) because

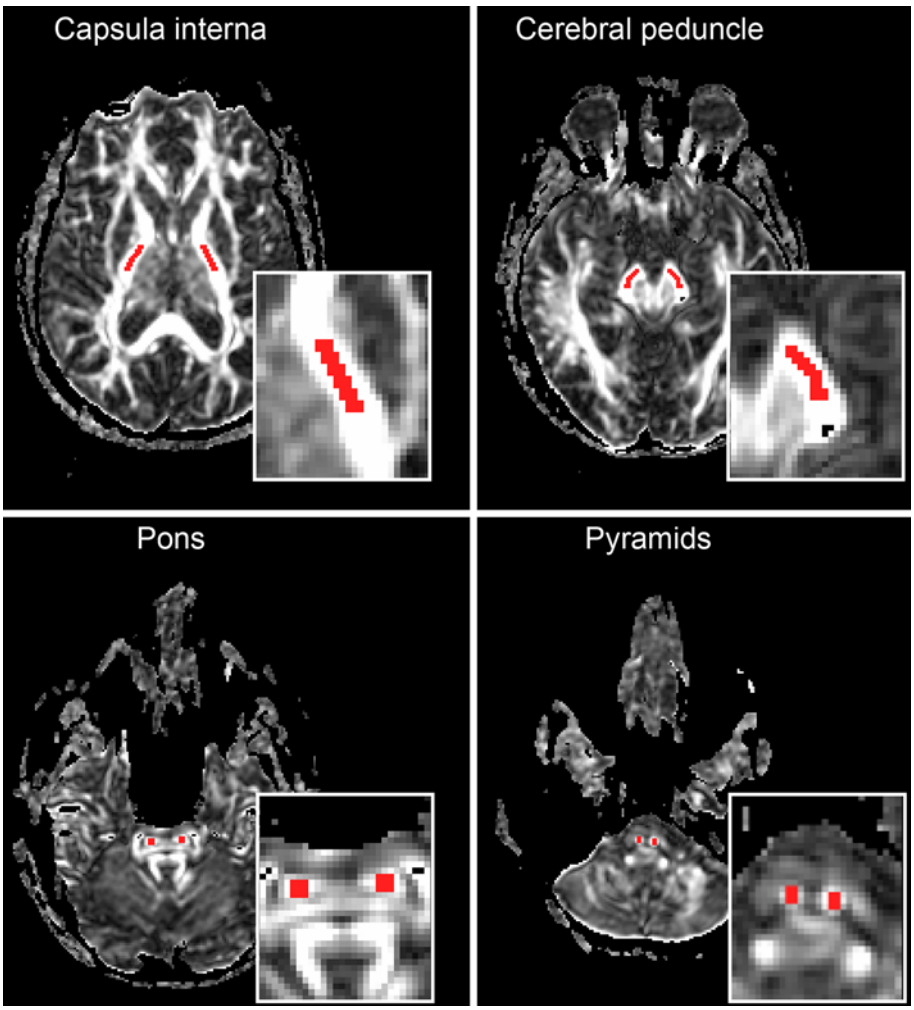


**Fig. 1** Fractional anisotropy maps at four different levels along the corticospinal tract. Regions of interest (ROIs) were placed on both sides of the capsula interna, cerebral peduncle, pons, and pyramids. Single mean apparent diffusion coefficient, fractional anisotropy, axial, and radial diffusivity were determined from the averaged values of the parameters in each ROI

MEPs could not be elicited (Table 2). On the initially affected sides, ulnar motor NCS showed reduced amplitudes in all and decreased NCV in two patients (no. 1 and 4). In two patients with an asymmetrical pattern (no. 1 and 3), the contralateral side was also affected. F-waves were reduced on the clinically affected side in four patients (no. 1, 2, 5, and 7), but not reliable ratable in two patients (no. 3 and 4). Sensory NCS were normal in all patients except one (no. 1) presenting deceased sensory NCV on the affected side. No abnormalities were found in the SSEP of the ulnar nerve in any patient. Sympathetic skin response was normal in six patients; it could not reliably be recorded in one (no. 4) (Table 3). Electromyography of the dorsal interossei muscles (hand) on the initially affected side showed pathological spontaneous activity in two (no. 2 and 6), reduced interference pattern in four (no. 1, 4, 5, and 6), and increased amplitudes (>5 mV) in three (no. 3, 5, and 7) patients indicating acute and chronic neurogenic remodeling. Signs of chronic neurogenic remodeling were also found on the contralateral, but clinically not affected side in two patients (no. 4 and 7). Five patients (no. 1, 2, 3, 6, and 7) additionally had neurogenic damage in the triceps brachii muscle. Electromyography of the tibialis anterior muscle was normal in all seven patients (Table 4).

## Diffusion tensor imaging analysis

Regions of interest-based diffusion parameters are summarized in Fig. 2 for HirD patients and controls at four different levels along the CST (capsula interna, cerebral peduncle, pons, and pyramids). For the control subjects, diffusion values of each region were averaged over the right and left brain hemisphere. Multivariate ANOVAs across all participants with the FA, ADC, AD, and RD values of each region (capsula interna, cerebral peduncle, pons, and pyramids) as dependent variables and with the factors [disease (control subjects, HirD), hemisphere (left, right), and side (affected, contralateral)] were performed respectively. These analyses revealed no significant main effect or significant interaction for any factor.

Based on CST tractography results, diffusion parameters were determined for the whole CST in all HirD patients

**Table 1** Demographical and clinical data of Hirayama disease patients

| | Patients | | | | | | |
|---|---|---|---|---|---|---|---|
| | 1 | 2 | 3 | 4 | 5 | 6 | 7 |
| Gender | F | F | M | M | M | M | M |
| Age (years) | 55 | 21 | 46 | 19 | 37 | 20 | 34 |
| Age at onset (years) | 17 | 14 | 17 | 16 | 18 | 14 | 12 |
| Progression (years) | >10 | 5 | L 3, R 2 | 3 | 5 | 5 | 12 |
| Height (cm) | 160 | 171 | 172 | 185 | 190 | 175 | 184 |
| Initially affected side | R > L | R | L > R | L | L | L > R | R |
| Atrophy[a] | R++ | R++ | L++, R+ | L++ | L+++ | L+++, R+ | R++ |
| Deep tendon reflexes lower limbs and Babisnkis sign (pyramidal tract signs) | Reflexes equal and active bilateral, no pyramidal tract signs | Reflexes equal and active bilateral, no pyramidal tract signs | Reflexes equal and active bilateral, no pyramidal tract signs | Patellar and ankle response hyperactive on left side, left ankle response clonic, Rossolimo reflex positive on left side | Reflexes equal and active bilateral, no pyramidal tract signs | Reflexes equal and active bilateral, no pyramidal tract signs | Reflexes equal and active bilateral, no pyramidal tract signs |
| Family history of muscle disease | None | None | None | None | Grandmother suspected for poliomyelitis | None | None |

*F* female, *M* male, *y* year, *L* left, *R* right

[a] Muscle atrophy: + = hand, ++ = hand and forearm, +++ = hand, forearm and arm

**Table 2** Motor evoked potentials in Hirayama disease patients

| | Patients | | | | | | | Normal lab value[a] |
|---|---|---|---|---|---|---|---|---|
| | 1 | 2 | 3 | 4 | 5 | 6 | 7 | |
| Right lower limb | | | | | | | | |
| MEP cortex latency (ms) | 23.6 | 24.2 | 26.0 | 25.6 | 30.4 | 29.2 | 29.2 | <30 |
| MEP spinal latency (ms) | 12.0 | NE | 12.8 | 10.8 | 15.6 | 12.8 | 12.4 | <15 |
| CMCT | 11.6 | | 13.2 | 14.8 | 14.8 | 16.4 | 16.8 | <18 |
| Left lower limb | | | | | | | | |
| MEP cortex latency (ms) | 23.2 | 24.6 | 26.0 | 28.0 | 30.4 | 29.2 | 29.2 | <30 |
| MEP spinal latency (ms) | 12.0 | NE | 12.8 | 10.8 | 12.8 | 12.8 | 12.8 | <15 |
| CMCT | 11.2 | | 13.2 | 17.2 | 17.6 | 16.4 | 16.4 | <18 |

*CMCT* central motor conduction time, *MEP* motor evoked potential, *NE* could not be elicited

[a] Reference values with standard neck positions

and control subjects (Table 5). Univariate ANOVAs across all participants with the FA, ADC, AD, and RD values of the CST as dependent variables and with the factors [disease (control subjects, HirD), hemisphere (left, right), and side (affected, contralateral)] were performed respectively. These analyses revealed no significant main effect or significant interaction for any factor.

Within the HirD patients, the relationship between CST diffusion parameters and the years of disease progression as well as age and CMCT were explored. We found a particularly high correlation between the RD of the CST with years of disease progression on the affected side ($r = 0.903$; $p = 0.005$) and on the contralateral side ($r = 0.787$; $p = 0.036$). Correlation tests did not identify any statistically significant relationship of the CST diffusion parameters with age and CMCT.

## Discussion

In this study, supraspinal CST fiber integrity of a well-defined larger group of HirD patients was investigated

**Table 3** Nerve conduction studies in Hirayama disease patients

| | Patients (initially affected side) | | | | | | |
|---|---|---|---|---|---|---|---|
| | 1 (R > L) | 2 (R) | 3 (L > R) | 4 (L) | 5 (L) | 6 (L > R) | 7 (R) |
| Ulnar nerve L (motor) | A↓ NCV↓ | N | A↓↓ dL↑ | A↓↓ NCV↓ dL↑ | A↓ | A↓ | N |
| Ulnar nerve R (motor) | A↓↓ NCV↓ | A↓ | A↓↓ dL↑ | N | N | N | A↓↓ |
| Ulnar nerve L F-waves | N | N | Ø | Ø | F↓ | N | N |
| Ulnar nerve R F-waves | F↓↓ | F↓ tDis | Ø | Ø | N | N | F↓↓ |
| Ulnar nerve L (sensory) | N | N | N | N | N | N | N |
| Ulnar nerve R (sensory) | NCV↓ | N | N | N | N | N | N |
| Ulnar nerve SSEP | NAL < R | N | N | N | N | N | N |
| Sympathetic skin response | N | N | N | Ø | N | N | N |

*A* amplitude (↓ decreased, ↑ increased), *dL* distal latency (↑ enhanced), *F* F-waves (↓ reduced persistence of F-waves, ↓↓ loss of F-waves), *L* left, *N* normal value, *NCV* nerve conduction velocity (↓ reduced), *R* right, *SSEP* somatosensory evoked potential, *tDis* temporal dispersion, Ø no reliable rating

**Table 4** Electromyography in Hirayama disease patients

| | Patients (initially affected side) | | | | | | |
|---|---|---|---|---|---|---|---|
| | 1 (R > L) | 2 (R) | 3 (L > R) | 4 (L) | 5 (L) | 6 (L > R) | 7 (R) |
| Dorsal interossei muscles (hand) L | Ripa↑ | N | A↑ | Ripa↑↑ | A↑ Ripa↑ | pSA Ripa↑↑ | A↑ |
| Dorsal interossei muscles (hand) R | Ripa↑↑↑ | pSA | A↑ | Ripa↑ | N | Ripa↑ | A↑ |
| Triceps brachii muscle L | Ripa↑ | N | pSA | N | Ø | pSA Ripa↑↑ | N |
| Triceps brachii muscle R | Ripa↑↑ | A↑ | N | N | N | Ripa↑↑ | A↑ |
| Tibialis anterior muscle L | N | N | N | N | N | N | N |
| Tibialis anterior muscle R | N | N | N | N | N | N | N |

*A*↑ increased amplitude, *L* left, *N* normal value, *Psa* pathological spontaneous activity, *R* right, *Ripa* reduced interference pattern (↑ moderate, ↑↑ clearly, ↑↑↑ very clearly), Ø no reliable rating

using DTI and TMS. The ROI-based and tract-specific diffusion parameters did not significantly differ between the initially affected and the contralateral side in HirD patients. There was also no difference when patients' initially affected side was compared to healthy controls. Three of the patients (no. 1, 3, and 6) studied here presented with bilateral, albeit asymmetric, wasting and weakness, which is in line with the clinical spectrum of reported HirD patients reflected in the designation of HirD as juvenile asymmetric segmental spinal muscular atrophy (JASSMA) [13]. The asymmetrical involvement of muscles contralateral to the first affected side has been reported in approximately 20 % of HirD cases and, furthermore, a new phenotype of bilaterally symmetric HirD has recently been described [27]. The missing differences of diffusion parameters within these patients are somehow explainable. In fact, it is surprising to find normal DTI parameters also in patients presenting pure unilateral symptoms. This finding argues against a supraspinal CST involvement in HirD and can instead be taken as positive evidence that HirD is a pure spinal motor neuron disorder.

We found a positive correlation between the RD of the CST and years of disease progression in both the affected and the contralateral side in HirD patients. Because the RD technically consists of an average of the two minor eigenvalues within the tensor ellipsoid, an increased diffusivity perpendicular to the main axon direction in patients with a longer disease progression could reflect a less coherently organized CST. In multiple sclerosis patients with chronic lesions, for example, an increased RD has been demonstrated to serve as a surrogate marker for dysmyelination and overall tissue integrity [28, 29]. Gallo et al. [30] postulated subtle CST alterations in a single HirD patient that might be masked by adaptive changes in white matter architecture due to cortical reorganization. The functional changes might play a compensatory role in limiting the clinical consequences of structural cord damage.

However, considering cervical cord damage at the lower motor neuron level, one would expect to find a pathological CMCT. In line with structural measures CMCT determined with TMS was normal in our HirD cohort, confirming previous reports [31–33]. In addition, MEPs did not show any alterations before and after neck flexion in earlier reports [12, 34].

Furthermore, fiber tractography, which offers a pathway-specific investigation remote from distally located

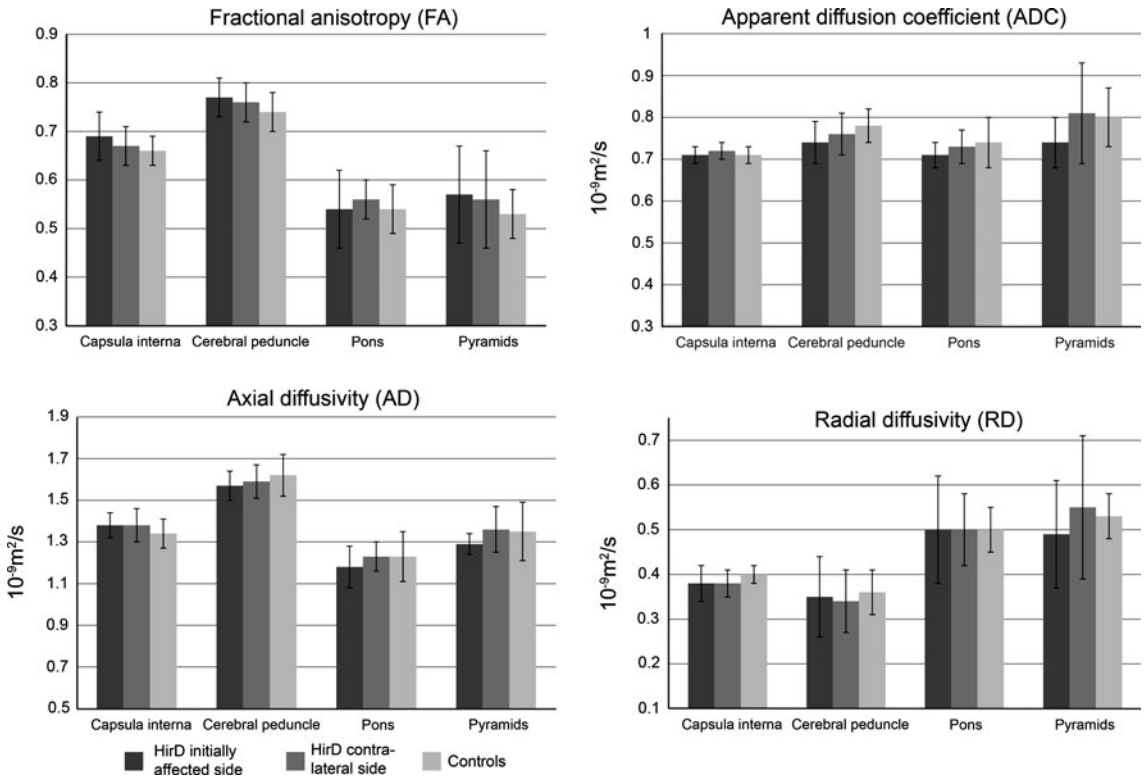


**Fig. 2** Region of interest-based corticospinal tract (CST) diffusion parameters. Mean diffusion parameters are presented along four representative levels of the CST (capsula interna, cerebral peduncle, pons, and pyramids), separated for diffusion coefficients: fractional anisotropy, apparent diffusion coefficient, axial diffusivity, and radial diffusivity. *Bars* in *dark grey* represent the HirD patients' initially affected side; *medium grey* represents HirD patients' contralateral side, and *light grey* healthy controls (averaged across the *left* and *right side*); *error bars* indicate standard deviation

**Table 5** Tract-specific diffusion parameters in corticospinal tract

| | Fractional anisotropy | | | Apparent diffusion coefficient ($10^{-9}m^2/s$) | | |
|---|---|---|---|---|---|---|
| Group | $HirD_{aff}$ | $HirD_{con}$ | $Con_{both}$ [a] | $HirD_{aff}$ | $HirD_{con}$ | $Con_{both}$ [a] |
| Mean (SD) | 0.46 (0.02) | 0.45 (0.03) | 0.43 (0.04) | 0.72 (0.02) | 0.72 (0.01) | 0.74 (0.02) |
| | Axial diffusivity ($10^{-9}m^2/s$) | | | Radial diffusivity ($10^{-9}m^2/s$) | | |
| Group | $HirD_{aff}$ | $HirD_{con}$ | $Con_{both}$ [a] | $HirD_{aff}$ | $HirD_{con}$ | $Con_{both}$ [a] |
| Mean (SD) | 1.12 (0.03) | 1.12 (0.03) | 1.12 (0.03) | 0.52 (0.02) | 0.53 (0.01) | 0.55 (0.03) |

*$HirD_{aff}$* patients initially affected side, *$HirD_{con}$* patients contralateral side, *$Con_{both}$* controls

[a] Averaged across left and right side

lesions, is sensitive enough to detect a secondary alteration of the CST in terms of a "dying-back" axonopathy. Retrograd fiber degeneration or shrinking of cortical representations following peripheral lesions have been frequently demonstrated. However, the absence of such a DTI signature is again indicative for an intact supraspinal pathway in HirD patients. In summary, structural and functional CST integrity was normal, so that no evidence for a supraspinal CST involvement in HirD was detected.

The DTI fingerprint of the CST in HirD patients can be used to differentiate HirD from other motor neuron diseases. In particular, patients with amyotrophic lateral sclerosis typically have significant FA reductions (especially in the posterior limb of the internal capsule) and an increase of ADC along the CST [35]. Damage of CST fibers reflects upper motor neuron degeneration. However, in progressive muscular atrophy, which represents a phenotype of amyotrophic lateral sclerosis without upper motor neuron involvement, DTI was normal [36]. It is thus not suitable to distinguish progressive muscular atrophy from HirD. In line with our data suggesting that HirD is a restricted spinal motor neuron disease without pyramidal tract involvement conventional MRI studies have commonly reported atrophic changes in the anterior cervical cord [10], consistent with neuropathology findings showing a loss of anterior horn cells without significant gliosis in this area [37]. Additionally, hyperintense signal alterations on T2-weighted images have been demonstrated in the anterior horns in HirD patients [7, 38].

However, the actual development of motor neuron lesioning leading to a characteristic phenotype in HirD is unidentified. The distribution of muscle atrophy does not perfectly match microcirculatory disturbances in the anterior spinal artery territory, thus alternative explanations for the focal cervical poliomyelopathy have to be considered. Assuming cord compression as a possible underlying cause, the organization of motoneuron groups and motor columns within the human cervical cord has to be considered [39]. At the cervical level, the ventral horn consists of lateral and dorsolateral subcolumns that innervate the dorsal and ventral parts of the limbs. Within these subcolumns, grouped motoneurons, so-called motor pools, are connected to individual muscles [40]. Thus, selected motor pools might be particularly vulnerable to repeated or sustained cervical cord compression. A selective degeneration within the columnar organization could also be caused by an intrinsic motoneuron disease. For instance, columnar degeneration is a typical scenario in poliomyelitis [41] and has also been postulated in patients with benign monomelic amyotrophy of the lower limb [42].

In summary, combined structural and functional measures imply normal integrity of the supraspinal CST in HirD patients supporting the notion that HirD is a pure spinal motor neuron disorder.

**Conflicts of interest** All authors declare no conflicts of interest in respect to the content of this article.

**Ethical standards** All human studies must state that they have been approved by the appropriate ethics committee and have therefore been performed in accordance with the ethical standards laid down in the 1964 Declaration of Helsinki.

## References


1. Hirayama K, Tsubaki T, Toyokura Y, Okinaka S (1963) Juvenile muscular atrophy of unilateral upper extremity. Neurology 13:373–380
2. Hirayama K (2000) Juvenile muscular atrophy of distal upper extremity (Hirayama disease). Intern Med 39:283–290
3. Tashiro K, Kikuchi S, Itoyama Y, Tokumaru Y, Sobue G, Mukai E, Akiguchi I, Nakashima K, Kira JI, Hirayama K (2006) Nationwide survey of juvenile muscular atrophy of distal upper extremity (Hirayama disease) in Japan. Amyotroph Lateral Scler 7:38–45
4. Gourie-Devi M, Suresh TG, Shankar SK (1984) Monomelic amyotrophy. Arch Neurol 41:388–394
5. Hashimoto O, Asada M, Ohta M, Kuroiwa Y (1976) Clinical observations of juvenile nonprogressive muscular atrophy localized in hand and forearm. J Neurol 211:105–110
6. Sakai K, Ono K, Okamoto Y, Murakami H, Yamada M (2011) Cervical flexion myelopathy in a patient showing apparent long tract signs: a severe form of Hirayama disease. Joint Bone Spine 78:316–318
7. Sonwalkar HA, Shah RS, Khan FK, Gupta AK, Bodhey NK, Vottath S, Purkayastha S (2008) Imaging features in Hirayama disease. Neurol India 56:22–26
8. Iwasaki Y, Tashiro K, Kikuchi S, Kitagawa M, Isu T, Abe H (1987) Cervical flexion myelopathy: a "tight dural canal mechanism". Case report. J Neurosurg 66:935–937
9. Konno S, Goto S, Murakami M, Mochizuki M, Motegi H, Moriya H (1997) Juvenile amyotrophy of the distal upper extremity: pathologic findings of the dura mater and surgical management. Spine 22:486–492
10. Chen CJ, Chen CM, Wu CL, Ro LS, Chen ST, Lee TH (1998) Hirayama disease: MR diagnosis. AJNR Am J Neuroradiol 19:365–368
11. Chen CJ, Hsu HL, Tseng YC, Lyu RK, Chen CM, Huang YC, Wang LJ, Wong YC, See LC (2004) Hirayama flexion myelopathy: neutral-position MR imaging findings—importance of loss of attachment. Radiology 231:39–44
12. Ammendola A, Gallo A, Iannaccone T, Tedeschi G (2008) Hirayama disease: three cases assessed by F wave, somatosensory and motor evoked potentials and magnetic resonance imaging not supporting flexion myelopathy. Neurol Sci 29:303–311
13. Willeit J, Kiechl S, Kiechl-Kohlendorfer U, Golaszewski S, Peer S, Poewe W (2001) Juvenile asymmetric segmental spinal muscular atrophy (Hirayama's disease): three cases without evidence of "flexion myelopathy". Acta Neurol Scand 104:320–322
14. Robberecht W, Aguirre T, Van den Bosch L, Theys P, Nees H, Cassiman JJ, Matthijs G (1997) Familial juvenile focal amyotrophy of the upper extremity (Hirayama disease). Superoxide dismutase 1 genotype and activity. Arch Neurol 54:46–50
15. Schroder R, Keller E, Flacke S, Schmidt S, Pohl C, Klockgether T, Schlegel U (1999) MRI findings in Hirayama's disease: flexion-induced cervical myelopathy or intrinsic motor neuron disease? J Neurol 246:1069–1074
16. Misra UK, Kalita J, Mishra VN, Phadke RV, Hadique A (2006) Effect of neck flexion on F wave, somatosensory evoked

potentials, and magnetic resonance imaging in Hirayama disease. J Neurol Neurosurg Psychiatry 77:695–698
17. Schlegel U, Jerusalem F, Tackmann W, Cordt A, Tsuda Y (1987) Benign juvenile focal muscular atrophy of upper extremities—a familial case. J Neurol Sci 80:351–353
18. Hirayama K (1991) Non-progressive juvenile spinal muscular atrophy of the distal upper limb (Hirayama disease). In: Jong JD (ed) Handbook of clinical neurology. Elsevier, Amsterdam, pp 107–120
19. Bodammer N, Kaufmann J, Kanowski M, Tempelmann C (2004) Eddy current correction in diffusion-weighted imaging using pairs of images acquired with opposite diffusion gradient polarity. Magn Reson Med 51:188–193
20. Papadakis NG, Xing D, Huang CL, Hall LD, Carpenter TA (1999) A comparative study of acquisition schemes for diffusion tensor imaging using MRI. J Magn Reson 137:67–82
21. Woods RP, Grafton ST, Holmes CJ, Cherry SR, Mazziotta JC (1998) Automated image registration: I general methods and intrasubject, intramodality validation. J Comput Assist Tomogr 22:139–152
22. Pajevic S, Pierpaoli C (1999) Color schemes to represent the orientation of anisotropic tissues from diffusion tensor data: application to white matter fiber tract mapping in the human brain. Magn Reson Med 42:526–540
23. Bodammer NC, Kaufmann J, Kanowski M, Tempelmann C (2009) Monte Carlo-based diffusion tensor tractography with a geometrically corrected voxel-centre connecting method. Phys Med Biol 54:1009–1033
24. Le Bihan D, Mangin JF, Poupon C, Clark CA, Pappata S, Molko N, Chabriat H (2001) Diffusion tensor imaging: concepts and applications. J Magn Reson Imaging 13:534–546
25. Mori S, Oishi K, Faria AV (2009) White matter atlases based on diffusion tensor imaging. Curr Opin Neurol 22:362–369
26. Glenn OA, Ludeman NA, Berman JI, Wu YW, Lu Y, Bartha AI, Vigneron DB, Chung SW, Ferriero DM, Barkovich AJ, Henry RG (2007) Diffusion tensor MR imaging tractography of the pyramidal tracts correlates with clinical motor function in children with congenital hemiparesis. AJNR Am J Neuroradiol 28:1796–1802
27. Pradhan S (2009) Bilaterally symmetric form of Hirayama disease. Neurology 72:2083–2089
28. Song SK, Sun SW, Ramsbottom MJ, Chang C, Russell J, Cross AH (2002) Dysmyelination revealed through MRI as increased radial (but unchanged axial) diffusion of water. Neuroimage 17:1429–1436
29. Klawiter EC, Schmidt RE, Trinkaus K, Liang HF, Budde MD, Naismith RT, Song SK, Cross AH, Benzinger TL (2011) Radial diffusivity predicts demyelination in ex vivo multiple sclerosis spinal cords. Neuroimage 55:1454–1460
30. Gallo A, Rocca MA, Tortorella P, Ammendola A, Tedeschi G, Filippi M (2006) A multiparametric brain and cord MR imaging study of a patient with Hirayama disease. AJNR Am J Neuroradiol 27:2115–2117
31. Misra UK, Kalita J (1995) Central motor conduction in Hirayama disease. Electroencephalogr Clin Neurophysiol 97:73–76
32. Rigamonti A, Usai S, Curone M, D'Amico D, Bussone G (2004) Hirayama disease: description of an Italian case. Neurol Sci 25:102–103
33. Polo A, Curro' Dossi M, Fiaschi A, Zanette GP, Rizzuto N (2003) Peripheral and segmental spinal abnormalities of median and ulnar somatosensory evoked potentials in Hirayama's disease. J Neurol Neurosurg Psychiatry 74:627–632
34. Chiba S, Yonekura K, Nonaka M, Imai T, Matumoto H, Wada T (2004) Advanced Hirayama disease with successful improvement of activities of daily living by operative reconstruction. Intern Med 43:79–81
35. Sach M, Winkler G, Glauche V, Liepert J, Heimbach B, Koch MA, Buchel C, Weiller C (2004) Diffusion tensor MRI of early upper motor neuron involvement in amyotrophic lateral sclerosis. Brain 127:340–350
36. Cosottini M, Giannelli M, Siciliano G, Lazzarotti G, Michelassi MC, Del Corona A, Bartolozzi C, Murri L (2005) Diffusion-tensor MR imaging of corticospinal tract in amyotrophic lateral sclerosis and progressive muscular atrophy. Radiology 237:258–264
37. Hirayama K, Tomonaga M, Kitano K, Yamada T, Kojima S, Arai K (1987) Focal cervical poliopathy causing juvenile muscular atrophy of distal upper extremity: a pathological study. J Neurol Neurosurg Psychiatry 50:285–290
38. Desai JA, Melanson M (2011) Teaching neuroimages: anterior horn cell hyperintensity in Hirayama disease. Neurology 77:e73
39. Routal RV, Pal GP (1999) A study of motoneuron groups and motor columns of the human spinal cord. J Anat 195:211–224
40. Romanes GJ (1964) The motor pools of the spinal cord. Prog Brain Res 11:93–119
41. Sharrard WJ (1955) The distribution of the permanent paralysis in the lower limb in poliomyelitis; a clinical and pathological study. J Bone Joint Surg Br 37:540–558
42. Munchau A, Rosenkranz T (2000) Benign monomelic amyotrophy of the lower limb—case report and brief review of the literature. Eur Neurol 43:238–240